Contribution from Ames Laboratory—ERDA and Department of Chemistry, Iowa State University, Ames, Iowa 50011

Zirconium Monobromide, a Second Double Metal Sheet Structure. Some Physical and Chemical Properties of the Metallic Zirconium Monochloride and Monobromide[1]

RICHARD L. DAAKE and JOHN D. CORBETT*

Received March 3, 1977 AIC70170+

Zirconium monobromide has been synthesized and shown from Guinier x-ray powder diffraction data to contain the same X–Zr–Zr–X slabs of four close-packed layers known in ZrCl but with an alternate packing of the four-layer slabs (ACB rather than ABC); $R = 0.16$ for 50 *hkl* reflections; $a = 3.5031$ (3) and $c = 28.071$ (3) Å for the trigonal cell $R\bar{3}m$. HfCl also occurs in the ZrBr structure; $a = 3.3697$ (3) and $c = 26.582$ (6) Å. The greater hardness of ZrBr, the absence of the graphitelike structural damage which ZrCl exhibits after grinding, and the relative distances in the two structures all appear to be manifestations of significantly stronger interslab binding in ZrBr. This is attributed to the presence of close, second nearest neighbor interactions between Br and Zr layers of the same orientation in adjoining slabs. The metallic character of both phases is clearly established by their x-ray photoelectron spectra, namely, the presence of a substantial density of occupied states at the Fermi level. Attempted intercalation reactions were unsuccessful for both phases.

Introduction

The synthesis of the zirconium and hafnium monochlorides was first achieved through extended reductions of first the respective tetrachlorides and then the reduced products therefrom with excess metal sheet at about 650 °C, utilizing the superior containment properties of tantalum to provide high purity products.[2] Other preparations of these two compounds have also been reported.[3,4] A totally new type of structure was subsequently deduced for ZrCl, a trigonal cell containing tightly bound double metal sheets between close packed halide layers to give the layering sequence Cl–Zr–Zr–Cl.[5] The present article reports the synthesis of the analogous ZrBr, the determination of its structure as a stacking variant of ZrCl, and some chemical and physical properties of the two monohalides. Subsequent publications will detail the utilization of these monohalide phases as convenient starting materials for the preparation of other less reduced zirconium chlorides and bromides.[6]

Experimental Section

Synthesis. Reactor-grade crystal bar zirconium (<500 ppm of Hf) was either cold-rolled to produce 0.4–0.5 mm sheets or strips or turned to 0.08–0.10 mm thick chips. The tetrachloride and tetrabromide were prepared by reaction of halogen vapor with excess metal strips at 400–450 °C, and the products were purified by vacuum sublimation ($<10^{-5}$ Torr) through a coarse grade Pyrex frit. Transfer and manipulation of these and the reduced halides were all carried out in a drybox filled with a prepurified nitrogen atmosphere which constantly recirculated through a column of molecular sieve. All subsequent reactions were performed in tantalum containers which had been sealed by arc welding under helium. For reactions generating appreciable pressure 13 or 19 mm o.d. tubing with 0.4 mm wall thickness was welded shut with 0.8 mm thick, formed Ta caps.

The first preparation and analytical identification of ZrBr was accomplished via two successive equilibrations of halide with excess Zr foil as described before[2] for ZrCl, since this procedure allows a clean separation of a new phase from excess reductant. Much larger amounts of both compounds were subsequently prepared quantitatively in a single container by reaction of heated metal turnings and the respective tetrahalide in stoichiometric proportions. The reaction temperature was raised slowly from 400 to 800–850 °C over a period of 1–2 weeks and maintained there for a few more days. Intermediate reaction pressures may have reached 30–40 atm judging from the bulging of the end caps on the container. The product was passed through a 100 mesh screen to remove any unreacted turnings (0.1% or less). Equilibrium dissociation pressures of $ZrX_4(g)$ above the Zr/ZrX systems were estimated (±10%) from experiments in which a crimped but not sealed 6-mm Ta tube containing ZrX was placed within a larger Ta tube of known free volume and the latter sealed. After equilibration for a few days the combination was quenched, back-reaction of ZrX_4 being reduced to substantially nil by its limited access into the inner container and the presence of 1–2 atm of He. The pressure in the outer tube at equilibrium was calculated from the results of a halide analysis of the ZrX_4 found therein and the free volume. Though $ZrX_3(g)$ likely represents a species in the equilibrium the amount is relatively small and not recognizable after quenching.

Analyses. All elemental analyses were performed by gravimetric techniques. Samples for halogen analysis were dissolved in 10–15 mL of 10% HF in stoppered polyethylene bottles to prevent loss of HX. The halides were determined gravimetrically as AgX after dilution with water and addition of acetone to facilitate coagulation. Analyses for Zr were performed by reaction of weighed ZrX samples with water vapor at 110 °C after which the resulting white product was ignited to ZrO_2. This latter method gives excellent results and avoids time-consuming precipitation and ignition procedures. Usual monohalide sample sizes were 0.3–0.4 g for X analyses and 0.4–0.6 g for Zr analyses. Recoveries (Zr + X) were typically between 99.8 and 100.0%.

XPS Data. X-ray photoelectron spectra of Zr, ZrCl, ZrBr, and $ZrCl_4$ were taken at Argonne National Laboratory on a McPherson ESCA 36 photoelectron spectrometer with a Mg Kα source. The unit had been modified for handling air- and moisture-sensitive compounds by attachment of an argon-filled drybox (2–6 ppm of H_2O and O_2). Measurements were made under a vacuum of $<10^{-9}$ Torr with a layer of gold vaporized onto potentially insulating samples for calibration. Ten-scan spectra were taken over 20-eV intervals at 111 points each.

X-Ray Data and Refinement. Powder diffraction data of excellent quality for high-precision line position measurements (± 0.005° in θ) were obtained with the evacuable Model XDC-700 Guinier camera (IRDAB, Stockholm) equipped with a quartz monochromator to provide a clean Cu Kα_1 incident beam. NBS Si powder was used as an internal standard. The photographic reproduction of a precision millimeter scale onto the front side of the film eliminated the need for a film shrinkage correction. The back side of the film was routinely covered with paper tape before developing to maximize line and scale sharpness and to minimize parallex in reading the film. Ground samples were mounted between two pieces of cellophane tape on a supporting washer in the drybox, and the assembly was transferred to the camera in a closed container. Even $ZrCl_3$ and $ZrBr_3$ give no visual or x-ray evidence of reaction with tape or air over several days as long as the exposure of the mounted sample to air during transfer to the camera is minimized (~5 s) and the sample stored in an evacuated container at other times.

In order to refine atom positions in the new ZrBr structure a high-quality Guinier film of that phase was scanned by a microdensitometer, and the relative integrated intensities were measured by weighing the peaks from the strip chart record. Thirty-six observed reflections out to $(\sin\theta)/\lambda = 0.45$ Å^{-1} were used plus 14 unobserved reflections which were put in at 40% of the weakest observed reflection. The intensity data were corrected for Guinier polarization and for multiplicity and the structure factors inputed into a standard ORFLS refinement in which the variables were the scale factor and the z coordinates of Br and Zr in general positions in space group $R\bar{3}m$ (trigonal cell). Initial values for the positions were z(Cl) and $^1/_3z$(Zr) from ZrCl, respectively.

Unit weights were used originally but the data were later reweighted in groups sorted by F_o so as to reflect better their relative precisions. Because of the laminar nature of ZrBr preferred orientation had always been a concern and its occurrence was verified by inspection of the data at an early stage ($R = 26\%$). Even though the sample had been

Chart I

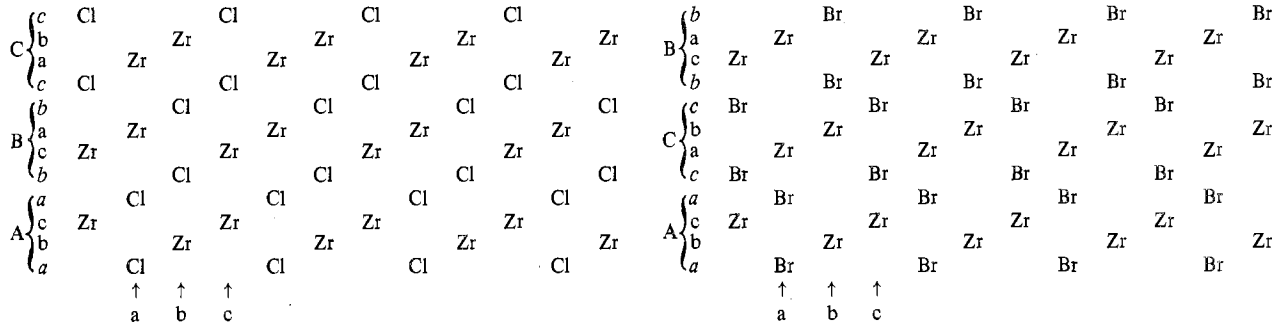

ground moderately well, it was clear that certain classes of reflections came into diffracting position less frequently in the Guinier experiment. The problem appeared to affect all 00*l* reflections plus *hkl* for $l \geq 10$ when $h + k = 1$ and for $l \geq 16$ when $h + k = 2$. This group of 22 (16 observed) reflections was given a single separate scale factor which refined to 70% of that for the remainder. Final converged parameters were $z(Zr) = 0.2092$ (4), $B = 0.5$ (4) Å^2 and $z(Br) = 0.3917(5)$, $B = 1.9$ (4) Å^2 with a conventional $R = 0.16$ (8.3 observations/variable). A separate refinement of occupancy together with positions showed that stacking defects corresponding to intergrowth of regions with ZrCl-type packing was apparently negligible (4 ± 3%). Two θ values for 23 well-resolved lines yielded trigonal cell parameters $a = 3.5031$ (3) and $c = 28.071$ (3) Å by least-squares refinement. All observed powder diffraction lines fell within 0.02° of the calculated 2θ values. A powder diffractometer scan of ZrBr was also made but refinement of these data was abandoned because of a substantially greater problem with preferred orientation.

Results

The compound ZrBr, like ZrCl, grows as black, reflective, hexagonal platelets. The rate of formation of crystals is slow enough that those of a size sufficient for single-crystal x-ray diffraction require reaction for several weeks at 850–900 °C. Analyses (for both elements) of samples of ZrBr prepared at 900 °C in the presence of a large excess of Zr foil gave 53.4 (±0.1)% Zr and 46.6 (±0.1)% Br (calcd 53.30% Zr, 46.70% Br). No x-ray evidence for a composition range in either ZrBr or ZrCl could be found, and all analyses were in the range X/Zr = 1.00 ± 0.01. Attempts to prepare ZrI by analogous means were all unsuccessful.

The thermal stabilities of these monohalides are quite remarkable. The equilibrium $ZrX_4(g)$ pressures are approximately 1 atm at 900 °C for both Zr/ZrCl and Zr/ZrBr systems and 2.9 atm at 975 °C for the former, based on recovery of ZrX_4 after quenching (see Experimental Section). The compounds also have unusually high melting points, that of ZrCl exceeding 1100 °C where the autogeneous pressure of $ZrCl_4(g)$ is ca. 15–20 atm.

The Crystal Structure of ZrBr. Guinier x-ray powder diffraction patterns of ZrBr contain more lines and are invariably sharper than those of ZrCl samples prepared under like conditions. Although a qualitative comparison of the powder patterns of ZrCl and ZrBr leads to the hypothesis that they are isostructural, a quantitative comparison of calculated intensities revealed some major discrepancies. Consideration of polytypism in some other layered compounds led to the determination of a different layering sequence for ZrBr.

The ZrBr structure, like that of ZrCl, consists of close packed layers each containing atoms of only one kind which repeat in the sequence X–Zr–Zr–X to generate four-layer slabs or sheets. Both compounds crystallize in the trigonal $R\bar{3}m$ space group with a 12 layer repeat in the *c* direction $(X–Zr–Zr–X)_3$ and with *a* equal to the nearest neighbor intralayer distance. The difference between the two structures comes from an alternative way of stacking the three four-layer slabs. This is depicted in Chart I in terms of the [110] section; the lower case letters *a*, *b*, *c* give the usual description of relative placement of horizontal layers when viewed along the vertical *c* axis. Thus the regular ···abc··· repeat in ZrCl gives four-layer slabs sequenced ABC (following the positioning of the X layers) and thence trigonal antiprismatic coordination of X with respect to M (same slab) and X (next slab). In the same notation ZrBr is ACB and each X is *trigonal prismatic* in coordination with respect to atoms in adjoining layers. Both structures have identical antiprismatic coordination of the metal atoms with respect to adjacent X and M layers within the slabs.

The x-ray intensity distributions for these two structural types are quite distinctive, as shown in Table I where the calculated intensities are compared with those observed for ZrBr. The positional coordinates of Zr and Br differ only slightly, but perhaps significantly, from those calculated for the ACB structure based on the ZrCl parameters. These and important distances in the zirconium monohalides are listed in Table II where they are compared with those of ScCl, which was subsequently shown by a single-crystal study[7] to be isostructural with ZrBr.

The analogous compound HfCl has been known for some time and was originally considered to be isotypic with the then unknown ZrCl structure from a comparison of powder data.[2] A more recent study[4] based on the correct cell and an only approximate[5] structure also concluded that the layer sequencing in HfCl was the same as in ZrCl, although intensities evidently were not considered. Calculations for HfCl in both sequences clearly show, much as in Table I, that HfCl adopts the ZrBr structure. Refined lattice constants for HfCl based on data obtained earlier[2] are given in Table III together with similar data for ZrCl, ZrBr, and other isotypic examples. The effect of a lanthanide contraction with HfCl is quite striking, particularly in the *a* dimension. On the other hand the change in structure type between ZrCl and HfCl apparently has a systematic effect on the *c* dimension (vide infra) so that the contraction is not as evident in that direction.

Chemical and Physical Properties. Layered and highly reduced compounds of this type might be expected to be excellent substrates for further chemical reactions. Although the subject phases readily react with H_2 to form some remarkable hydride phases[9,10] attempts at intercalation reactions along the lines well known for the layered transition metal disulfides[11] have all been negative, as judged principally by the lack of any swelling or detectable change in lattice parameters. Reactants tested include liquids pyridine (ZrCl and ZrBr, 7 weeks, 115 °C), NH_3 (ZrBr, 8 days, 23 °C), N_2H_4 (ZrBr, 4 days, 23 °C), and triphenylphosphine (ZrBr, 10 days, 300 °C), gaseous Al_2Cl_6 (ZrCl, 21 weeks, 120 °C), and I_2 in CCl_4 (ZrCl, 5 h, 25 °C).

The strongly bonded double layers of zirconium atoms sandwiched by sheets of well-bonded halogen atoms give rise to a number of properties commensurate with such anisotropic bonding. The strong bonding within the slabs is manifest in their high thermal stabilities and melting points above 1100 °C. Both phases have a high reflectivity and are in appearance

Table I. Observed Guinier Powder Diffraction Intensities for ZrBr and Their Calculated Values Based on ACB and ABC (ZrCl) Packing (Cu Kα)

hkl	*d*(calcd),[a] A	I_{calcd}[a] ACB	I_{obs}[b]	I_{calcd}[c] ABC
003	9.36	20	14	11
006	4.68	14	8	13
009	3.119	0	0	0
101	3.016	8	15	0
012	2.965	19	17	1
104	2.785	3	9	100
015	2.669	100	100	1
107	2.419	24	19	5
0,0,12	2.339	11	8	11
018	2.295	0	0	47
1,0,10	2.066	36	30	11
0,1,11	1.953	5	3	7
0,0,15	1.871	6	5	3
1,0,13	1.759	2	3	0
110	1.752	30	50	30
113	1.722	1	8	1
0,1,14	1.673	0	0	9
116	1.640	4	11	5
0,0,18	1.560	2	1	3
119	1.527	0	0	0
1,0,16	1.519	3	5	6
021	1.515	1	0	0
202	1.508	3	11	0
024	1.483	0	0	18
205	1.464	16	38	0
0,1,17	1.450	10	8	0
027	1.419	5	11	1
1,1,12	1.402	14	21	17
208	1.392	0	0	12
0,0,21	1.337	1	0	1
0,2,10	1.334	10	13	3
1,0,19	1.328	0	0	6
2,0,11	1.304	1	1	2
1,1,15	1.279	11	17	8
0,1,20	1.274	2	1	2
0,2,13	1.241	1	1	0
2,0,14	1.210	0	0	5
1,0,22	1.176	6	4	5
0,0,24	1.170	0	0	0
1,1,18	1.165	5	4	10
0,2,16	1.148	1	1	4
211	1.146	1	1	0
122	1.143	3	5	0
0,1,23	1.132	5	2	5
214	1.132	1	0	23
125	1.124	19	29	0
2,0,17	1.117	6	2	0
217	1.102	6	6	2
128	1.090	0	0	19
0,2,19	1.058	0	0	5
1,0,25	1.053	0	0	4

[a] Based on refined values of cell and position parameters. [b] A modest amount of preferred orientation is present, giving low observed intensities for 00*l* reflections and for *hkl* with large *l* (see Experimental Section). [c] Based on positional parameters for ZrCl.[5]

as well as cleavage reminiscent of graphite. In fact the characteristic effect of sample grinding on the powder pattern of ZrCl, in marked contrast to that of ZrBr, is similar to that known[12] for some graphites where the defects produced evidently amount to random translation and rotation of layers relative to one another around c^*. This leads to the development of broad diffuse bands connecting *hkl* reflections with the same values of $h + k$ ($h + k \neq 0$), an effect which is particularly pronounced in ZrCl through the groups of reflections 101–015, 110–116, 024–027, and 214–217 while 00*l* reflections remain sharp.

The levels of intrinsic stacking defects in ZrCl and ZrBr vary in a similar manner. There is no evidence to speak of for line broadening in ZrBr on grinding, whereas different samples of unground ZrCl show an appreciable range of line broadening effects of the character generally associated with displacement (deformation) defects.[12] In view of the proclivity of ZrCl to grinding damage it is not surprising that the sharpest patterns come from fine powders which have been equilibrated at high temperatures and screened but not ground. The broadest lines in the best patterns obtained (104, 110) are only about twice as wide as lines of similar angle and intensity from ZrBr. Selected "single" crystals of ZrCl grown under a wide variety of conditions show exceedingly diverse qualities related to disorder. The best give good Weissenberg patterns with sharp unstreaked spots, although a great deal of effort is necessary to locate such examples.[5] Other may give streaks even 5–7 mm long in the Weissenberg pattern for all reflections, 00*l* as well as *hkl*, suggesting a broad and fairly smooth distribution of defects in the stacking direction as well as between layers. Intergrowth with ZrBr-type layering at an irregular level could be responsible for the latter, but intensity anomalies are not evident between sharp and badly streaked (zero level) films.

Table II. Distances (A), Angles (deg), and Atomic *z* Coordinates in the Double-Layered Structures of ZrCl, ZrBr, and ScCl

		ZrCl[a]	ZrBr	ScCl[b]
Intralayer distance	M-M, X-X	3.424 (2)	3.5031 (3)	3.473 (2)
Interlayer distance	M-M	3.087 (5)	3.130 (12)	3.216 (6)
	X-X	3.607 (14)	3.85 (2)	3.695 (8)
	M-X	2.629 (6)	2.74 (1)	2.591 (4)
∠M-M-M[c]			68.0 (2)	65.3 (1)
∠M-X-M[c]			79.5 (4)	84.1 (2)
z(M)		0.1220 (1)	0.2092 (4)	0.2137 (1)
z(X)		0.3901 (3)	0.3917 (5)	0.3914 (1)

[a] Reference 5. [b] ZrBr-type structure.[7] [c] Interlayer angle.

Table III. Lattice Constants (Trigonal Cell) for the Double-Layered Monohalides

Compd	*N*[a]	*a*, A	*c*, A	*c*/*a*	Type	Source
ZrBr	23	3.5031 (3)	28.071 (3)	8.01	ZrBr	This work
HfCl	24	3.3697 (3)	26.582 (6)	7.89	ZrBr	This work
ZrCl	16	3.424 (2)	26.57 (4)	7.76	ZrCl	Ref 5
	10	3.4233 (5)	26.693 (3)	7.80		This work
ScCl	13	3.473 (2)	26.71 (4)	7.69	ZrBr	Ref 7
GdCl		3.819 (1)	27.482 (6)	7.20	ZrCl	Ref 8
TbCl		3.787 (1)	27.461 (5)	7.25	ZrCl	Ref 8

[a] Number of indexed reflections used in refinement.

Both ZrCl and ZrBr are rather ductile and small pellets may be pressed at 7 Mg/cm^2 and room temperature to 97% of the theoretical density. These exhibit resistances of <0.1 Ω through a few millimeters by simple dc methods (VTVM), although the reactivity, laminar nature, and small size of single crystals available all mitigate against direct measurements of their presumably highly anisotropic conductivity. Using larger crystals Troyanov[13] found (by an unspecified method) resistivities of about 2×10^{-2} Ω cm within ZrCl platelets and 10^3 Ω cm normal to them (c axis[5]). But the x-ray photoelectron spectra of both ZrCl and ZrBr, Figure 1, provide a ready and relatively unambiguous proof that these phases are metallic in that they clearly exhibit a valence d band with a substantial density of occupied states at the Fermi level. Some core level data for the monohalides as well as for Zr and $ZrCl_4$ are also listed in Table IV. Both core and valence levels for zirconium and chlorine show plausible chemical shifts with oxidation state in the series Zr–ZrCl(ZrBr)–$ZrCl_4$. The principal orbital contributions assigned to the ZrCl bands in Figure 1 as well as the observed energies are in good agreement with the results of unpublished (self-consistent KKR) band calculations by Marchiando, Harmon, and Liu.[15] The ZrBr structure does appear to exhibit slight (0.3 eV) but consistently

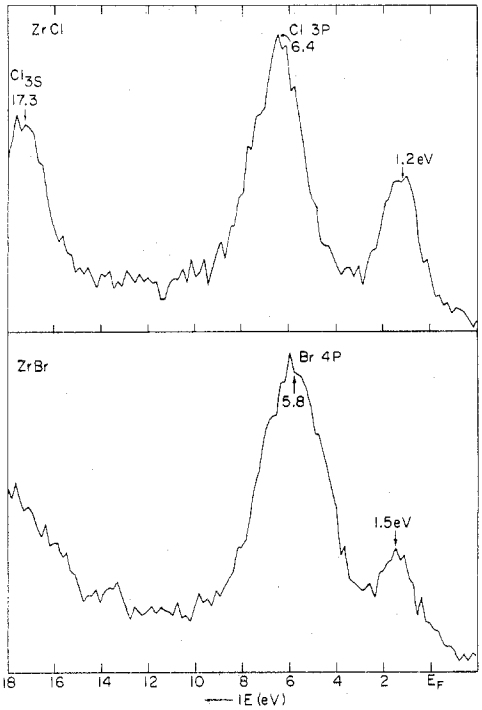

Figure 1. X-ray photoelectron spectra of the valence region of ZrCl (top) and ZrBr (bottom) (unsmoothed data, ten scans).

Table IV. X-Ray Photoelectron Spectra for Some Zirconium Halides, eV

Level	Zr	ZrBr	ZrCl	$ZrCl_4$[a]
Zr "4d"		1.5	1.2	
Br 4p		5.8		
Cl 3p			6.4	5.0
Cl 3s			17.3	15.7
Zr $3d_{5/2}$	177.6[b]	179.6	179.3	182.8[b]
Zr $3d_{3/2}$[c]	180.0	182.0	181.8	185.2
Br $3p_{3/2}$		182.6		
Br $3p_{1/2}$		189.9		
Cl $2p_{3/2}$			199.6	198.5
Cl $2p_{1/2}$			201.2	200.1

[a] Corrected for charging (−1.8 eV) based on measurements of Au $4f_{7/2,5/2}$ levels from metal vaporized onto sample. [b] Reference 14 gives Zr $3d_{5/2}$ as 178.5 and 182.8 eV for Zr and $ZrCl_4$, respectively, relative to C (1s) from adventitious hydrocarbons at 285.0 eV. [c] Only small O (1s) peaks were observed on reduced samples as were small peaks or shoulders at ~185.4 eV (Zr $3d_{3/2}$), which compare with 185.6 eV for this level in ZrO_2 on Zr.

higher binding energies for the metal in both the valence and core regions. The zirconium monohalides (as well as $HfCl^2$) exhibit a Pauli-type paramagnetism at room temperature which is appropriate to the density of states at E_F implied by Figure 1, $10^6\chi_M$(cor) being +97 and +107 emu/mol for ZrCl and ZrBr at 300 K, and ~5% greater at 50 K with no evidence of a phase transition to 4 K.[16]

Discussion

Properties of the zirconium monohalides vary appropriately between those reflective of strong bonding between the double zirconium sheets (3.09–3.13 Å vs. 3.18 and 3.23 Å in α-Zr) and those arising from the weak interaction at van der Waals distances between the X–Zr–Zr–X slabs or sheets. The first is evidenced by chemical reactions of the metal sandwich, such as hydride formation, while the latter gives rise to graphitelike cleavage or disorder between slabs. Both of these aspects prompt further investigation.

The *reason* for the formation of these double metal layer structures is by no means obvious, though the arrangement does offer a recognized advantage[17] in preserving the very strong metal–metal bonding present in the element itself. These two ways of packing the three four-layer slabs with the same repeat period (*c* axis), ABC (ZrCl) vs. ACB (ZrBr), do present a nomenclature problem in their comparison. A minimally acceptable solution seems to be *polytypic*, though that usage has generally pertained to a single compound which forms structures with differing layering sequences *and* repeat periods. At present a dimorphism of a single compound which spans both the ZrCl and ZrBr structure types is not known, so application of the polytypism classification to these two types must also neglect the difference in halogen involved.

Some factors responsible for differentation of the two structures may be inferred from their properties. The most striking, the greater strength and minimal number of stacking defects in ZrBr in the "weak" direction, must arise from the fact that the interlayer trigonal prismatic coordination of Br allows each Zr to "see" a second nearest bromine layer through an interstice in the first, viz.

$$X_aZr_bZr_cX_a|X_cZr_aZr_bX_c|X_bZr_cZr_aX_b|$$

In ZrCl this effect is lost as the second and third slabs are interchanged, leaving one to wonder why the ZrCl arrangement forms at all. Interlayer arrangements giving second nearest neighbor configurations quite analogous to ZrBr and ZrCl occur with $CdCl_2$ vs. CdI_2, respectively, but here it is the metal in the more "ionic" $CdCl_2$ which supposedly benefits from the additional second nearest neighbor chlorine. A subtle redistribution of charge in between the double metal sheets in ZrX may also occur on the switch from chlorine to the larger bromine as the structure expands in the *a* direction in order to keep the metal period commensurate with that in the close-packed anion layer. However, the expansion in *a* from ZrCl to ZrBr is only 0.08 Å (3.42 – 3.50 Å, Table II), leaving Br–Br contacts 0.42 Å less than twice the usually accepted van der Waals radius (1.96 Å), a notable amount even for halogen atoms bound to common high-field cations. The 0.24 Å expansion in the interlayer X–X distances from ZrCl to ZrBr is a little less than the expected difference of 0.30 Å but not as striking. Both of these effects would be consistent with a polarized, nonspherical bromide ion. Interestingly, a different polarization in ZrCl (and CdI_2) may be effective in reducing repulsion between anion layers.[7] With the regular ···abc··· sequencing in ZrCl, strings of Zr–Cl–Cl–Zr atoms occur in the [1$\bar{1}$6] and equivalent directions in the pseudo-close-packed planes. It appears that polarization of Cl by high-field Zr would induce a less negative charge on the opposite side of the anion adjacent to the second halide, and vice versa. A combination of electrostatic and polarization effects on the change of anion thus appears to be important in the structural differentiation between the two layering modes. The possible existence of these or related effects in $CdCl_2$ vs. CdI_2 has been also commented on in rather different terms by Krebs.[18]

Other indications of a significant difference between ZrCl and ZrBr in the details of the bonding in the double Zr–Zr sheets can be inferred from the metal–metal distances, the lattice dimensions, and the XPS results. The intralayer expansion on conversion from chloride to bromide does not result in a greater interpenetration of the two Zr layers and a constant interlayer Zr–Zr distance but rather the zirconium–zirconium separation actually appears to increase 0.04 Å (3.3σ) (Table II), perhaps in response to the attraction of the second nearest neighbor bromide now present in the other slab (vide supra). The same effects may be responsible for the consistently larger *c*/*a* ratio for compounds in the same periodic group which have the ZrBr structure, Table III. In a similar way both the (primarily) d valence band and the

zirconium core levels measured by XPS are slightly (0.3 eV) but consistently more tightly bound in ZrBr, contrary to expectations based on electronegativity. Again, the additional electrostatic interaction discussed above, related changes with the metallic bands, or both may be responsible.

Acknowledgment. The authors are indebted to Dr. Mirtha Umaña for measurement of the XP spectra of ZrCl, ZrBr, and related compounds, to Dr. R. J. Thorn for the use of the instrument, and to Dr. F. J. DiSalvo for the magnetic susceptibility measurements.

Registry No. ZrBr, 31483-18-8; ZrCl, 14989-34-5; HfCl, 25516-75-0; $ZrCl_4$, 10026-11-6; Zr, 7440-67-7.

References and Notes

(1) Work was performed for the U.S. Energy Research and Development Administration under Contract No. W-7405-eng-82.
(2) A. W. Struss and J. D. Corbett, *Inorg. Chem.*, **9**, 1373 (1970).
(3) S. I. Troyanov and V. I. Tsirel'nikov, *Russ. J. Inorg. Chem. (Engl. Transl.)*, **15**, 1762 (1970).
(4) A. S. Izmailovich, S. I. Troyanov, and V. I. Tsirel'nikov, *Russ. J. Inorg. Chem. (Engl. Transl.)*, **19**, 1597 (1974).
(5) D. G. Adolphson and J. D. Corbett, *Inorg. Chem.*, **15**, 1820 (1976).
(6) R. L. Daake and J. D. Corbett, to be submitted for publication.
(7) K. R. Poeppelmeier and J. D. Corbett, *Inorg. Chem.*, **16**, 294 (1977).
(8) A. Simon, H. Mattausch, and N. Holzer, *Angew. Chem.*, **88**, 685 (1976).
(9) A. W. Struss and J. D. Corbett, *Inorg. Chem.*, **16**, 360 (1977).
(10) T. Y. Hwang, A. W. Struss, R. G. Barnes, and D. R. Torgeson, unpublished research.
(11) F. R. Gamble, J. H. Osiecki, M. Cais, R. Pisharody, F. J. DiSalvo, and T. H. Geballe, *Science*, **174**, 493 (1971).
(12) A. J. C. Wilson, "X-Ray Optics", 2nd ed, Methuen and Co., Ltd., London, England, 1962, Chapter 6.
(13) S. I. Troyanov, *Vestn. Mosk. Univ., Khim.*, **28**, 369 (1973).
(14) V. I. Nefedov, Y. V. Salyn', A. A. Chertkov, and L. N. Padurets, *Zh. Neorg. Khim.*, **19**, 1443 (1974).
(15) J. Marchiando, B. N. Harmon, and S. H. Liu, unpublished calculations.
(16) F. J. DiSalvo, private communication.
(17) H. Schäfer and H. G. Schnering, *Angew Chem.*, **76**, 833 (1964).
(18) H. Krebs, "Fundamentals of Inorganic Crystal Chemistry", McGraw-Hill, London, 1968, p 227.

Contribution from the Department of Chemistry, Oakland University, Rochester, Michigan 48063

Hydrogen Bonding. 8. Preparation, Properties, and Low-Temperature Infrared Structural Analysis of Ammonium and Alkylammonium Trihydrogen Tetrafluorides and Tetramethylammonium Dihydrogen Trifluoride[1,2]

IRENE GENNICK,[3a] KENNETH M. HARMON,* and MARY M. POTVIN[3b]

Received December 13, 1976 AIC608744

Trialkylammonium trihydrogen tetrafluorides are extremely stable species in which the cation is hydrogen bonded to the central fluoride of a C_{3v} $H_3F_4^-$ anion; these zwitterionic liquid complexes resist loss of hydrogen fluoride even at elevated temperatures and can be distilled intact. Ammonium and methyl- and dimethylammonium ions form similar complexes with additional hydrogen bonding from extra cation hydrogens to terminal fluorines in the anion. The structure of these compounds accounts for the unusual stability order of acid fluoride complexes of hydrogen-bond donor cations relative to alkali metal cations; in each series the highest complex species stable at room temperature is one in which the central fluoride is coordinatively saturated with four hydrogen bonds. The broad, diffuse room-temperature infrared spectra of these complexes are completely resolved at 12 K and show in addition to bands of the cationic and anionic species an intense set of bands in the 2900–2300-cm^{-1} region. These anomalous bands are combination bands formed by intramolecular coupling of the H–F and F–F stretching frequencies. The low-temperature infrared spectrum of the C_{2v} $H_2F_3^-$ anion in tetramethylammonium dihydrogen trifluoride shows similar combination bands, which shift on deuterium substitution.

Introduction

The literature poses an interesting question concerning the relative stability of complex acid fluoride anions: with simple cations such as sodium,[4,5] potassium,[6-8] rubidium,[9,10] and cesium[10,11] the order of anion stability is $H_4F_5^- < H_3F_4^- < H_2F_3^- < HF_2^-$; however, with the hydrogen-bond donor cations hydronium[12] and ammonium[13-15] the observed order is $H_3F_4^- < HF_2^-$, and no compounds containing either $H_4F_5^-$ or $H_2F_3^-$ anions are found.

The alkali metal series, as represented by the potassium ion salts, has been described well; the crystal structures of potassium hydrogen difluoride,[16] dihydrogen trifluoride,[17] and tetrahydrogen pentafluoride[18] show the anions in these salts to be of $D_{\infty h}$, C_{2v}, and T_d symmetries, respectively, when packing modifications are neglected, and we have recently determined[2,19] that the $H_3F_4^-$ anion in potassium trihydrogen tetrafluoride has C_{3v} symmetry through correlation of anion structures with low-temperature infrared spectra for potassium dihydrogen trifluoride, trihydrogen tetrafluoride, and tetrahydrogen pentafluoride. Thus the HF_2^-, $H_2F_3^-$, $H_3F_4^-$, and $H_4F_5^-$ ions in potassium ion salts are formed by successive hydrogen bonding of one, two, three, and four hydrogen fluorides to a central fluoride ion. The structures of the four anions are shown in Figure 1, and the formulas and melting points of the complex acid fluorides of the alkali metals, with the exception of lithium which only forms a hydrogen difluoride, are listed in Table I.

Table I. Stoichiometries and Melting Points of Alkali Metal Complex Acid Fluorides

Cation	Mp, °C				Ref
	HF_2^-	$H_2F_3^-$	$H_3F_4^-$	$H_4F_5^-$	
Na^+	~270 dec	*a*	61.6[b]	38.8	4, 5
K^+	239	71.7	65.8	72	7
Rb^+	205	61.5	51	30[c]	9
Cs^+	176	50.2	32.6	*d*	11

[a] Not available. [b] Incongruent. [c] RbF·7HF (mp – 77.3 °C, incongruent) also found. [d] CsF·6HF (mp –42.3°) also found.

The stoichiometries of the complex acid fluorides of hydronium and ammonium ions have been established by detailed thermochemical studies. Cady and Hildebrand[12] studied the freezing point diagram of the water–hydrogen fluoride system and showed that the only compounds to form were $H_3O^+F^-$ (mp –35.5 °C), $H_3O^+HF_2^-$ (mp –75.6 °C), and $H_3O^+H_3F_4^-$ (mp –100.4 °C). There was no indication of $H_2F_3^-$ or $H_4F_5^-$ species. Westrum and co-workers[13,14] carried out a calorimetric study of the ammonia–hydrogen fluoride system with similar results; the only compounds that exist in this system are $NH_4^+F^-$ (decomposes), $NH_4^+HF_2^-$ (mp 126.2 °C), and